

Diabetic Complications Consortium

Application Title: Mitochondrial mechanisms of epigenetic dysregulation in diabetic gastroparesis

Principal Investigator: Tamas Ordog, M.D.

1. Project Accomplishments:

Epigenetic effects of dysregulated mitochondrial metabolism have recently been recognized in cancers with mutations in subunits A-D of the tricarboxylic acid (TCA) cycle and electron transfer chain enzyme complex succinate dehydrogenase (SDH) and in the TCA cycle enzyme isocitrate dehydrogenase (Kaelin & McKnight, *Cell* 2013; 153: 56-69). For example, loss-of-function mutations in SDH subunits can cause the inhibition of at least 17 Jumonji C (JmjC) domain-containing histone demethylases (Højfeldt *et al.*, *Nat Rev Drug Discov* 2013; 12: 917-30) and TET1/2/3 DNA demethylases (Killian *et al.*, *Cancer Discov* 2013; 3: 648-57) via competition with their cofactor α -ketoglutarate (2KG) by elevated succinate (SU) levels. SU levels are also elevated in diabetes (Peti-Peterdi, *Kidney Int* 2010; 78: 214-7) but their epigenetic effects remain unclear. In this project we aimed to investigate the hypothesis that ICC depletion in diabetic gastroparesis is related to SU-induced epigenetic repression of genes required for the maintenance and function of interstitial cells of Cajal (ICC). Using 3 strains of transgenic mice with genomic deletion of SDH subunit C (*Sdhc*) we have demonstrated that maintenance of ICC and normal gastric emptying depend on normal SDH function. We have shown that SU/2KG ratios are elevated in the stomach of patients with diabetes, and that reproducing these metabolic changes in KIT⁺, KIT-dependent cells derived from human gastrointestinal stromal tumors (GIST), which originate from ICC, by RNA interference-mediated knockdown of *SDHB* leads to downregulation of KIT protein levels via increased binding to the *KIT* promoter of repressive histone marks normally controlled by JmjC domain-containing histone demethylases. In this model we have also found increased DNA methylation in the *KIT* promoter and enhancers located within, and upstream of, *KIT* in both mouse ICC and human GIST cells. Finally, we have provided proof of the concept that interfering with *Ezh2*, the enzyme that establishes two of the repressive histone marks we found to be elevated in response to *SDHB* knockdown can prevent or reverse gastric ICC loss due to age-related transcriptional repression of *Kit* transcription in mice. We have published one paper in the high-impact journal *Gastroenterology* and a second paper is under revision for resubmission to a cell biology journal. Furthermore, data generated through this project supported a successful competitive renewal of a long-standing NIH/NIDDK grant (DK058185).

2. Specific Aims:

Specific Aim 1. Identify succinate as a metabolic link to epigenetic repression of ICC genes in diabetes.

Results:

Hypothesis 1: Succinate dehydrogenase is required for ICC maintenance.

To demonstrate that the mitochondrial tricarboxylic acid (TCA) cycle metabolite succinate (SU) is elevated in the stomach in diabetes, we performed gas chromatography and mass spectrometry (GC/MS) in gastric *tunica muscularis* tissues from female diabetic and matched nondiabetic patients. SU levels were normalized to α -ketoglutarate (2KG), another TCA cycle metabolite, which is required for proper functioning of a host of Jumonji C (JmjC) domain-containing histone demethylases and TET1/2/3 DNA demethylases and whose effects as a cofactor are inhibited competitively by SU. SU/2KG ratios were elevated in diabetic tissues (10.2 ± 3.6 vs. 4.6 ± 0.6 ; $n=3$). To examine the effects of elevated SU/2KG ratios on ICC and ICC functions, we studied 3 different mouse models with genomic deletions disabling the SU metabolizing enzyme complex succinate dehydrogenase (SDH). SDH subunit C (*Sdhc*) was inactivated by inducing cre-mediated recombination globally in $Tg^{CAG-creERT2}; Sdhc^{fl/-}$ and $R26^{M2rtTA/+}; Tg^{tetO-cre}; Sdhc^{fl/fl}$ mice and in a Kit-specific manner in $Kit^{creERT2/+}; Sdhc^{fl/fl}$ mice. In $R26^{M2rtTA/+}; Tg^{tetO-cre}; Sdhc^{fl/fl}$ mice wherein *Sdhc* had been inactivated by 20-day oral tetracyclin treatment, gastric SDHC protein levels were reduced to nearly undetectable levels as expected. By Western blotting we detected downregulation of the ICC marker proteins KIT and ETV1 and ERK1/2 phosphorylation, an indicator of KIT activity and a key mechanism of ETV1 stabilization (**Fig. 1A; see next page**). In $Tg^{CAG-creERT2/+}; Sdhc^{fl/-}$ mice treated with long-term tamoxifen to activate creERT2, loss of SDHC protein was associated with reduced ICC and ICC stem cells (ICC-SC) by flow cytometry (FCM) in the stomach (**Fig. 1B**), ileum, and distal colon, and with reduced KIT and ETV1 protein levels and reduced ERK1/2 phosphorylation in the jejunum. KIT^+ANO1^+ ICC networks were depleted in the jejunum and proximal colon. More recently we examined the effects of ICC-specific *Sdhc* genomic deletion in $Kit^{creERT2}$ mice. After a 3-day tamoxifen treatment, similarly to the findings in the other two models, we detected reduced KIT and ETV1 levels and reduced ERK1/2 MAP kinase activation in the stomach and depleted KIT^+ANO1^+ ICC networks in the colon (**Fig. 1C**). Gastric emptying of solids determined by breath test was delayed at 5 weeks post-induction ($T_{1/2}$ median: 136 min; IQR: 124-160 min). Long-term evaluation of gastric emptying is underway. These results strongly indicate that elevated SU/2KG ratios seen in diabetes reduce ICC and may delay gastric emptying of solids.

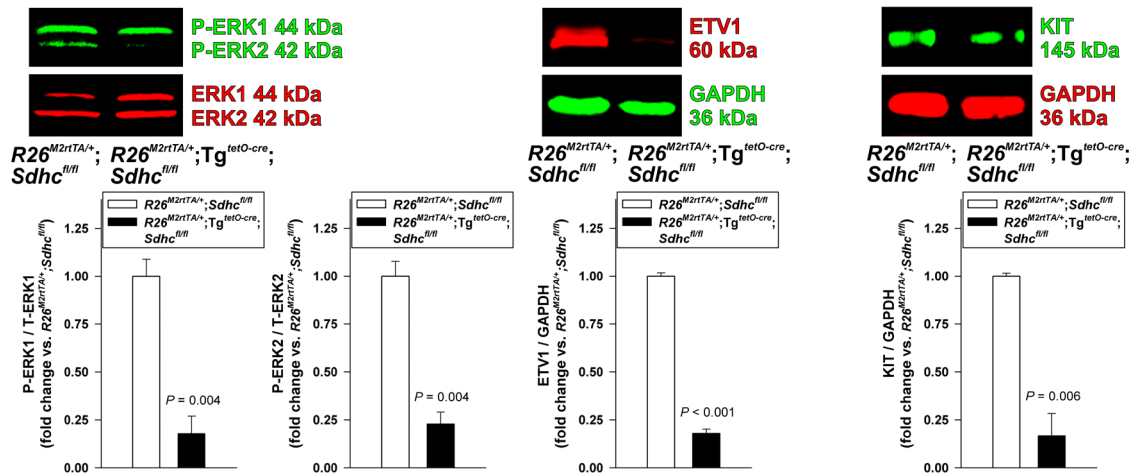


Fig. 1A. Effects of conditional genomic deletion of *Sdhc* on ERK1-ERK2 phosphorylation and ETV1 and KIT protein levels analyzed by WB in the gastric corpus+antrum *tunica muscularis* of doxycyclin-treated $R26^{M2rtTA/+};Tg^{tetO-cre};Sdhc^{fl/fl}$ and $R26^{M2rtTA/+};Sdhc^{fl/fl}$ controls. *Sdhc* deletion reduced ERK1-ERK2 phosphorylation and ETV1 and KIT protein levels (n=5-6/group).

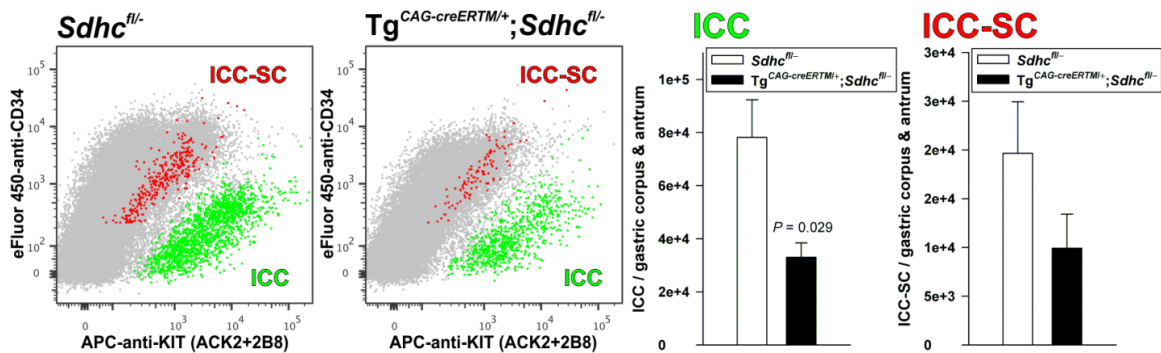


Fig. 1B. Effects of conditional genomic deletion of *Sdhc* on ICC and ICC-SC enumerated by flow cytometry in the gastric corpus+antrum *tunica muscularis* of tamoxifen-treated $Tg^{CAG-creERTM/+};Sdhc^{fl/-}$ mice and age- and sex-matched control $Sdhc^{fl/-}$ mice. ICC (KIT^+CD34^- cells; green) and ICC-SC ($KIT^{low}CD34^+$ cells; red) detected in the non-hematopoietic, $CD44^+$ fraction (grey) of gastric muscles were reduced in *Sdhc*-deleted mice vs. controls (n=4/group).

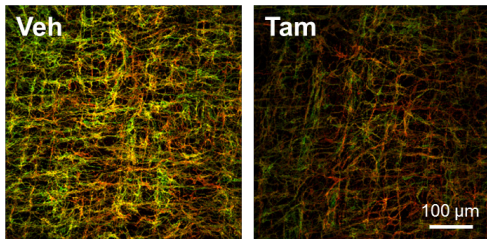


Fig. 1C. Effect of conditional deletion of *Sdhc* on KIT^+ (green) and $ANO1^+$ (red) ICC networks (overlays are shown) in the colon of $Kit^{creERT2/+};Sdhc^{fl/fl}$ mice (n=4 mice/group) 20 weeks post-induction with tamoxifen. ICC networks were depleted in the *Sdhc*-deleted mice.

Hypothesis 2: Succinate accumulation regulates gene transcription in ICC by inhibiting α -ketoglutarate-dependent “erasers” of epigenetic marks.

Since KIT⁺ ICC cannot be continuously maintained *in vitro*, we performed mechanistic experiments in a human KIT⁺ GIST cell line (GIST-T1) used as a human ICC model. We successfully knocked down *SDHB* (verified by Western blot) with 3 of the 4 different Dharmacon siRNAs tested (25 nM, 3 days; control: scrambled sequences). In GIST-T1 cells, following *SDHB* knockdown using the most effective siRNA and scrambled sequences as control (n=3/group) we verified increased SU (7.7±0.5 vs. 5.4±0.1 pmol/μg protein; *P*=0.011) and reduced 2KG levels (0.21±0.04 vs. 0.64±0.17 pmol/μg protein), as well as increased SU/2K ratios (37.7±4.0 vs. 10.2±3.4; *P*=0.006) by GC/MS. *SDHB* knockdown also reduced KIT protein levels to 29% (median; IQR: 6-63%) of control (*P*=0.029; n=4 per group). To examine the role of histone demethylases in the SU-mediated repression of *KIT* expression, we analyzed the levels of 6 methylated histone marks with established roles in the regulation of gene transcription. In response to *SDHB* knockdown, levels of the repressive marks H3K27me3, H3K9me3 and H3K9me2 increased significantly (fold change>1.5; *P*<0.05; n=7/group), whereas levels of the weakly repressive mark H3K27me2 and the activating marks H3K4me3 and H3K36me3 did not change significantly. In preliminary chromatin immunoprecipitation-sequencing (ChIP-seq) experiments we detected increased occupancy of the *KIT* promoter in response to *SDHB* knockdown; the verification of this finding in an independent study is underway (sequencing has been completed; bioinformatic analysis is ongoing). Next, we studied whether increased DNA methylation could also contribute to *KIT* repression in response to SU accumulation. We performed reduced representation bisulfite sequencing (RRBS), which detects both methylated and hydroxymethylated cytosines, and TET-assisted RRBS (TABs), which only detects hydroxymethylated cytosines. CpG dinucleotides with greater than 10% increase in true methylation were concentrated in the *KIT* promoter's CpG island and 300-350 kilobases upstream of the *KIT* transcription start site (**Fig. 2; see next page**). To understand the function of these sites, we performed ChIP-seq on the enhancer-associated histone mark acetylated H3K27 in GIST cells and also in colonic and small intestinal ICC purified by FACS. These experiments indicated that CpGs gaining methylation were associated with enhancers and super-enhancers shared by ICC and GIST cells. Together, our studies revealed histone- and DNA-methylation-mediated epigenetic repression of the key ICC gene *KIT* by elevated SU/2KG ratios characteristic of diabetes.

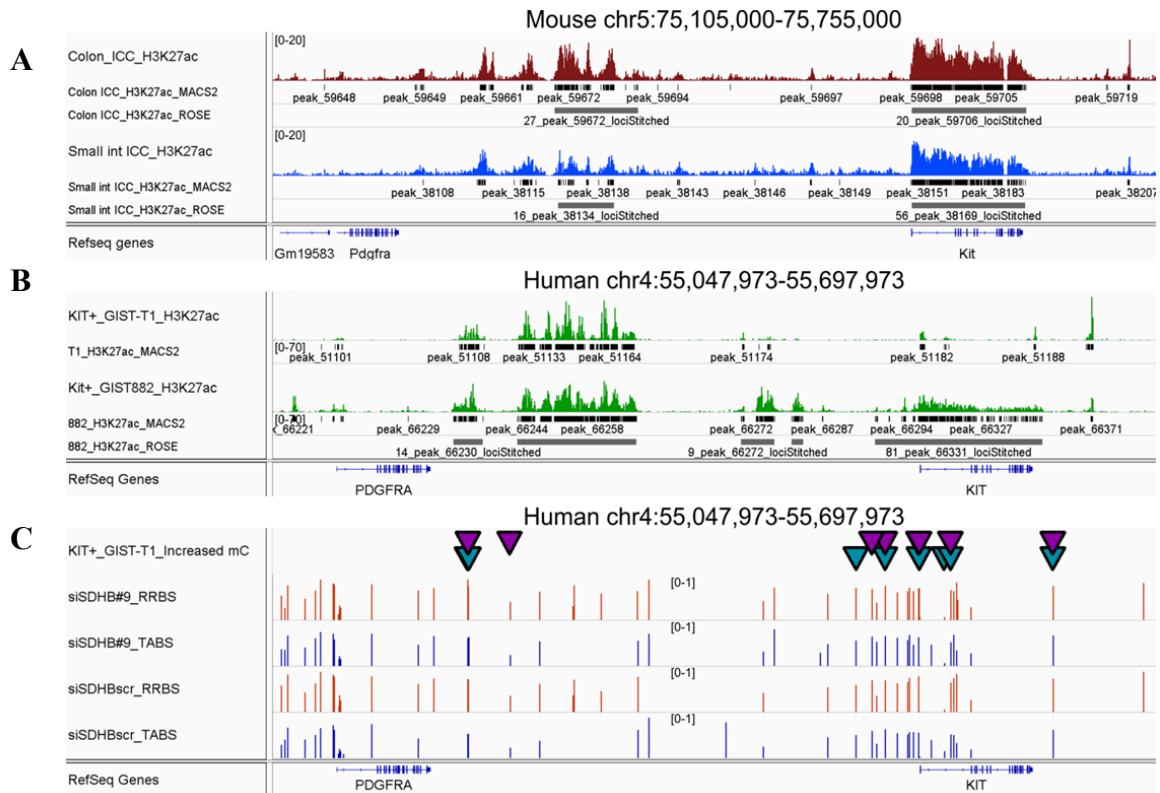


Fig. 2. *SDHB* knockdown increases CpG methylation in super-enhancers of the *PDGFRA-KIT* locus. H3K27ac occupancy (A) of the mouse *Pdgfra-Kit* locus (650 kb) in colonic and small intestinal ICC harvested from 4-8-wk-old *Kit^{CreERT2/+};R26^{mt-mG}* mice <1 week after tamoxifen-induced recombination by FACS and (B) in the corresponding region in KIT⁺ GIST-T1 and GIST882 cells (green). Black horizontal bars are significant peaks detected by *MACS2*; gray bars are super-enhancers identified by *ROSE*. (C) Fractional CpG methylation and hydroxymethylation detected by RRBS (5mC+5hmC) and TABS (5hmC) in GIST-T1 cells transfected with si*SDHB* #9 or scrambled sequences. CpGs with >10% increase in 5mC, shown by dark cyan (forward strand) and purple triangles (reverse strand), were predominantly located in super-enhancers.

Hypothesis 3: Inhibition of “writers” of repressive epigenetic marks mitigates the transcriptional effects of succinate accumulation.

Maintenance of epigenetic marks depends on the balance of their “writers” and “erasers”. It is not feasible at this time to re-activate “erasers” that may be inhibited by metabolic dysregulation. Therefore, we hypothesized that the effects of succinate-inhibited histone and DNA demethylases can be countered by inhibiting their “writers”. First, we performed proof-of-concept experiments aimed to determine the effects of ICC lineage-specific in-vivo deletion of *Ezh2*, the “writer” of the repressive histone marks H3K27me2/3, which limits the differentiation of Kit^{low} ICC-SC and facilitates the dedifferentiation of Kit⁺ ICC into Kit^{low} post-functional ICC (post-ICC) in postnatal mice by repressing *Kit* expression. Genomic deletion of *Ezh2* in *Kit*-transcribing cells was induced in *Kit^{creERT2/+};Ezh2^{fl/fl}* mice by 3 consecutive doses of tamoxifen (0.075 mg/g b.wt. i.p.) between 3-5 months of age, when ICC numbers dramatically decline in the murine stomach. FCM analysis of dissociated gastric *tunica muscularis* tissues indicated

a reduction in both Kit^{low} ICC-SC and Kit^{low} post-ICC, resulting in reduced ICC-SC/ICC and post-ICC/ICC ratios (**Fig. 3A,B**). These results signify that Ezh2 inhibition can indeed facilitate ICC differentiation and reverse/prevent ICC dedifferentiation. Experiments involving pharmacological inhibition of Ezh2, DNA methylation and H3K9 methylation in mice with ICC-specific conditional deletion of *Sdhc* are underway.

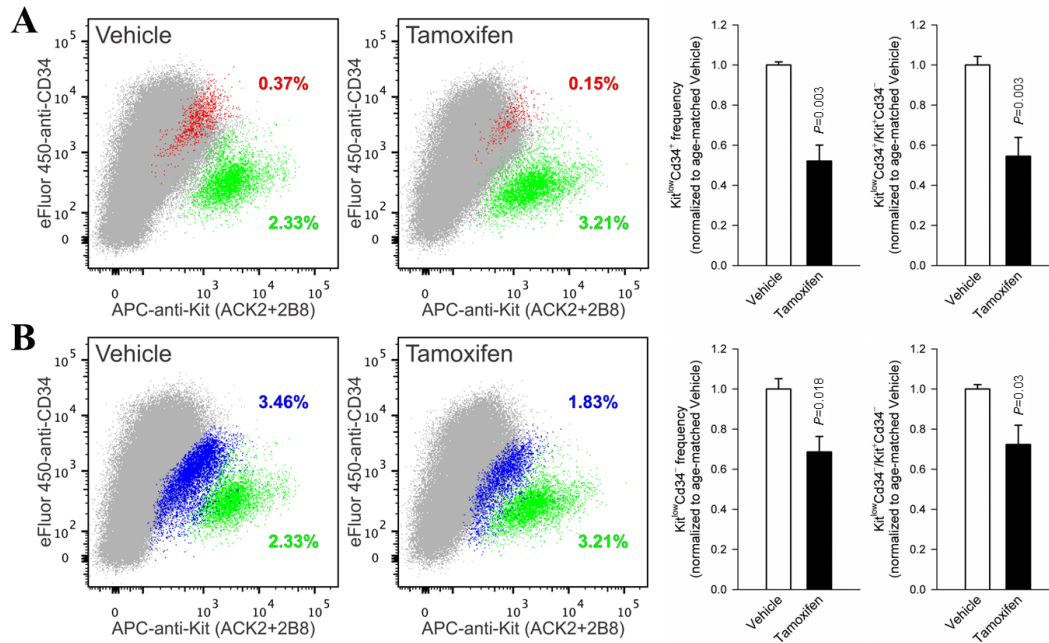


Fig. 3. ICC lineage-specific conditional deletion of *Ezh2* facilitates the differentiation of Kit⁺ ICC from Kit^{low} ICC-SC (**A**) and prevents/reverses ICC dedifferentiation into Kit^{low} post-ICC (**B**). Left panels show FCM profiles of 100,000 dissociated gastric *tunica muscularis* cells from a representative vehicle-treated and a tamoxifen-treated mouse. ICC (KIT⁺CD34⁺ cells; green), ICC-SC (KIT^{low}CD34⁺ cells; red) and post-ICC (KIT^{low}CD34⁻; blue) were detected in the non-hematopoietic fraction (grey) of gastric muscles. Percentages are cell frequencies of the total live cell population. Bar graphs show ICC-SC and post-ICC frequencies (left graphs) and ICC-SC/ICC and post-ICC/ICC ratios (right graphs) in tamoxifen-treated mice (n=7) normalized to the vehicle-treated group (n=5).

3. Publications:

Full paper:

Hayashi Y, Toyomasu Y, Saravanaperumal SA, Bardsley MR, Smestad JA, Lorincz A, Eisenman ST, Cipriani G, Nelson Holte MH, Al Khazal FJ, Syed SA, Gajdos GB, Choi KM, Stoltz GJ, Miller KE, Kendrick ML, Rubin BP, Gibbons SJ, Bharucha AE, Linden DR, Maher LJ 3rd, Farrugia G, **Ordog T.** Hyperglycemia Increases Interstitial Cells of Cajal via MAPK1 and MAPK3 Signaling to ETV1 and KIT, Leading to Rapid Gastric Emptying. *Gastroenterology* 2017 Aug; 153 (2):521-535.e20 Epub 2017 Apr 21 PMID: 28438610 PMCID: 5526732 DOI: 10.1053/j.gastro.2017.04.020

Published abstracts:

Saravanaperumal SA, Hayashi Y, Gajdos GB, Clark CR, Zhang W, Nelson Holte MH, Nie J, Gaonkar KS, Yan H, Maher LJ III, Lee JH, **Ordog T**. Succinate dehydrogenase regulates kit expression and interstitial cells of Cajal (ICC). *Neurogastroenterol Motil* 2016; 28:107

Saravanaperumal SA, Hayashi Y, Gajdos GB, Syed SA, Clark CR, Smestad JA, Nelson Holte MH, Al Khazal FJ, Miller KE, Linden DR, Kendrick ML, McKenzie TJ, Kellogg TA, Gaonkar KS, Yan H, Baheti S, Sun Z, Saur D, Farrugia G, Lee JH, Maher III LJ, **Ordog T**. Succinate accumulation epigenetically represses KIT expression, reduces interstitial cells of Cajal (ICC) and delays gastric emptying of solids. *Gastroenterology* 2017; 152:(5)S129-30. Abstract no. 593.